The Egyptian Journal of Hospital Medicine (October 2022) Vol. 89 (2), Page 6637- 6645

Developing Gold-Resveratrol Nanoconjugates for Management of Rheumatoid Arthritis (RA)

Marwa Dawood Jaaffer[1*], Israa Ali Zaidan Al-Ogaidi[2]

[1,2]Department of Biotechnology, College of Science, University of Baghdad, Bagdad, Iraq

Corresponding auther: Marwa Dawood Jaaffer**, Moblie**: +9647708214513**, Email:** Marwa.Jaafer1106@sc.uobaghdad.edu.iq

ABSTRACT

Introduction: The development of nanotechnology, due to the unique physical and chemical features of nanomaterials. Nanomaterial therapy for RA can increase bioavailability and target damaged joint tissue

Objective: This study aimed to check the effect of gold nanoparticles (AuNPs) with resveratrol by polyethylene glycol to manage the levels of ten immune markers of rheumatoid arthritis patients.

Patients and Methods: Gold nanoparticles (AuNPs) were functionalized with resveratrol by polyethylene glycol and utilized to manage the levels of 10 immune markers of 84 rheumatoid arthritis patients and 20 healthy volunteers ranging in age from 18 to 80 years.

Results: The synthesized gold nanoparticles, before and after functionalization, were characterized by UV-Vis spectrophotometer, Fourier-transforms spectroscopy, zeta potential, and FE-SEM. The levels of 10 immune markers in the sera of RA patients (IgA, IgE, IgG, RF, ANA, anti-dsDNA, C3, C4, IL-6, and IL-33) were tested by ELISA kits to study the *in vitro* effects of treatment with functionalized and non-functionalized AuNPs on their immune response.

Conclusion: The levels of all markers were decreased significantly in RA patients after exposure to AuNPs or AuNPs-PEG-Res. However, the levels of IgE, RF, ANA, dsDNA, C3, C4, and IL-33 showed significantly higher reduction in the presence of AuNPs as compared to AuNPs-PEG-Res, whereas the opposite was observed for the levels of IgA, IgG, and IL-6.

Keyword: Nanotechnology, Gold nanoparticles (AuNPs), Resveratrol (Res), Rheumatoid arthritis (RA), ELISA**.**

INTRODUCTION

Rheumatoid arthritis (RA) is a chronic autoimmune systemic disease that primarily damages the lining of synovial joints. It causes progressive disability, premature death, and has a significant economic impact [(1)]. It is critical to understand how pathologic mechanisms lead to the deterioration of RA progression in individuals in order to design medicines that effectively treat patients at each stage of their disease [(2)]. The mainstay of RA treatment is still pharmacologic therapy, which includes traditional, biological, and cutting-edge potential small molecular disease-modifying anti-rheumatic drugs. Significant progress has been made toward disease recovery without joint deformity. However, a sizable minority of RA patients do not respond well to currently available treatments. The available medication specifically targets macrophage proliferation and the production of pro-inflammatory cytokines. The therapeutic effectiveness of current treatment options at the targeted site is limited. Therefore, there is a pressing need to develop a new therapeutic method that could give more targeted drug delivery and make it safer [(3)].

Resveratrol (Res) is a plant polyphenol molecule that has trans-Res capability for cancer protection [(4)]. The most well-known polyphenolic stilbenoid is resveratrol, which can be found in raisins, mulberries, peanuts, and rhubarb [(5)]. Resveratrol may be beneficial for preventing the progression of chronic inflammatory diseases such as diabetes, obesity, cardiovascular disease, neurodegeneration, and cancer [(6)]. **Yahfoufi *et al.* [(7)]** found that resveratrol also affects immunity by messing with the way immune cells work, how proinflammatory cytokines are made, and how genes are expressed.

Nanotechnology is becoming increasingly essential in modern research. Nanotechnology is concerned with the development and utilization of materials with dimensions smaller than 100 nm, which are referred to as nanomaterial [(8)]. Nanomaterial has a greater surface-to-volume ratio, allowing them to perform well in a variety of applications such as Nano sensors, Nano-sorbents, and fuel cells [(9)]. Gold compounds have been used to treat RA for more than 50 years, dating back to Jacques Forestier's [(10)] discoveries in the early 1930s. Recently, AuNPs have been used to carry materials like DNA, peptides, anticancer drugs, and antibody products [(11)]. It is known that the properties vary according to the size, shape, medium, cell type, charge, and nanoparticle synthesis reduction agent [(12)]. It's important to study the effects of AuNPs on their own before putting them together with other drugs. This will help find the best way to use them in therapy.

Some previous studies of nanoparticles trying to control the RA disease. GNPs/MTX-Cys-FA Nano-conjugates for RA targeted therapy methods are studied by **Li *et al.* [(13)]**. By decreasing the expression and secretion of inflammatory factors, GNPs/MTX-Cys-FA can drastically reduce rheumatoid synovitis and successfully protect articular cartilage. **Yang *et al.* [(14)]** found that resveratrol had anti-inflammatory properties reducing

Received: 2/7/2022
Accepted: 8/9/2022

synovial tissue ROS buildup, inflammation, and angiogenesis both *in vivo* and *in vitro*. Furthermore, resveratrol's anti-inflammatory, anti-angiogenic, cytostatic, and pro-apoptotic effects are likely due to its inhibition of MAPK signaling pathways. In this sense, resveratrol has enormous promise as a treatment for RA.

Therefore, research based on nanomaterial has a reflective impact within medical science. The development of therapeutic inorganic nanoparticles is a crucial aspect of nanomedicine. The importance of NPs in medicine and biology has risen dramatically in recent years. However, nothing is known regarding their impact on rheumatic diseases treatment [(15)].

PATIENTS AND METHODS

This study included the collection of residual sera from 84 patients and 20 healthy volunteers from Iraq/Baghdad's Dowaly Private Hospital and Medical City/Educational Laboratories during the period from June to September 2021. Patients' blood samples were taken in tubes. Serum was taken out of blood by centrifuging and kept in small amounts at -4 °C until time of test.

Preparation of gold nanoparticle (AuNPs)

The method described by **Turkevich *et al.*** [(16)] was used to synthesize AuNPs; a volume of 100 mL of 1 mgml $^{-1}$ trisodium citrate solution was heated to 100°C to make AuNPs with a nanoscale diameter of 20 nm. Following that, 2 mL of 5 mgml^{-1} HAuCl4.H2O solution was promptly added to the trisodium citrate solution while vigorously stirring at 100 °C. After 10 minutes, the solution's color changed to red wine, followed by the formation of AuNPs. The solution was then allowed to cool down to room temperature while being constantly stirred.

Preparation of gold nanoparticle functionalized resveratrol (AuNPs-PEG-Res)

Gold nanoparticle functionalize resveratrol (AuNPs-PEG-Res) was carried out using 15 mL of AuNPs, stirred while it was still warm. 2.175 ml of 0.04 mM aqueous PEG was added while stirring. To obtain Res-conjugated AuNPs-PEG, 3.425 mL of aqueous Res (made by dissolving 0.5 mg of Res powder in 15 mL of D.W) was dropped into the mixture dropwise, and stirring at 150 rpm continued for 2 hours at 40°C (AuNPs-PEG-Res) [(17)].

Characterization of AuNPs and AuNPs-PEG-Res

The reduction of AuNPs and AuNPs-PEG-Res Utilizing a U-2910 spectrophotometer, ions were examined (Hitachi, Japan). Continuous scanning between 200 and 600 nm in wavelength was used to perform UV–vis spectroscopic analysis. The AuNPs and AuNPs-PEG-Res solutions were next examined using an X-ray diffractometer (XRD-6000, Shimadzu, Japan). A Cu K incident beam (= 1.542 A°) at 2θ = 20°–60° was used to generate the diffraction pattern. The X-ray tubes' voltage and current were 40 kV and 30 mA, respectively. The size was determined using the Debye-Scherrer equation, $D = 0.94 \lambda / \beta \cos \theta$. The FTIR analysis was carried out utilizing an FTIR spectrometer (8400S, Shimadzu, Japan), which has a resolution of 4 cm^{-1} and a spectral range of 4000-400 cm-^{1}. Finally, there was FE-SEM (Shimadzu AA-7000, Japan).

Indirect ELISA protocol

Standard serial diluted solutions were made. The following concentrations of immunoglobulin's (IgA, IgE, IgG): (1000, 250, 62.5, 15.6, 3.9, 0.89, 0.24, 0 ng/ml), (0, 50, 150, 373, and 1250 ng/ml), (100, 50, 25, 12.5, 6.25, 3.13, 1.56, and 0 ng/ml) respectively. After dispensing 100 µl of samples and standards into pre-assigned wells, the plate was incubated for 2 hours at 37°C, and each well was washed three times with 200 µl of wash buffer per well. After washing, 100 µl of AuNPs and AuNPs-PEG-Res were dispensed in each well, and the plate was incubated for 120 minutes at 37°C before being washed twice. After washing, 100 µl of HRP-conjugate was placed in each well, and the plate was incubated at 37°C for 60 minutes. After washing, TMB substrate (90 µl) was spread in each well, and blue colors of varying densities developed in the wells within 15–30 minutes. The reaction was then stopped by adding 50 µl of stop solution, causing the wells to turn yellow. Finally, the absorbance was read at 405 nm.

Sandwich ELISA protocol

Standard serial diluted solutions were made complement compounds (C3,C4) and interleukins (IL-6,IL-33) concentrations were prepared at (300, 150, 75, 37.5, 18.75, 9.4, 4.7, and 0 ng/ml), (300, 100, 33.3, 11.1, 3.7, 1.23, 0.41, and 0 ng/ml), (500, 250, 125, 62.5, 31.2, 15.6, 7.8, and 0 ng/ml), (1000, 500, 250, 125, 62.5, 31.2, 15.6, and 0 ng/ml) respectively. 100 µl of samples and standards into pre-assigned wells and the plate was incubated for 2 hours at 37°C.

After incubation, the contents of the wells were removed, and each well was washed twice with 200 µl of wash buffer per well. Following washing, 100 µl of AuNPs and AuNPs-PEG-Res were dispensed into each well, and the plate was incubated at 37°C for 120 minutes before being washed twice. After washing, 100 µl of HRP-conjugate was placed in each well, and the plate was incubated at 37°C for 60 minutes. After washing, TMB substrate (90 µl) was spread in each well, and blue colors of varying densities developed in the wells within 15–30 minutes. The reaction was then stopped by adding 50 µl

of stop solution, causing the wells to turn yellow. Finally, the absorbance was read at 405 nm.

Ethical Consideration:

Baghdad University Ethics Board approved the study. The Declaration of Helsinki, the code of ethics of the World Medical Association, was followed when conducting this research on humans. Every patient gave a written informed consent for participation in the study.

Statistical analysis

The data were coded, processed, and analyzed using the Statistical Package for Social Sciences (SPSS) version 22 for Windows (IBM SPSS Inc., Chicago, IL, USA). Quantitative information was presented as mean SD (Standard deviation), independent groups of normally distributed variables were compared using the one-way ANOVA. P value ≤ 0.05 was regarded as significant.

RESULTS

Preparation of gold nanoparticles (AuNPs)

In 1951, **Turkevich *et al.*** [16] proposed that tetrachloroauric acid might be reduced by trisodium citrate at high temperatures to produce gold nanoparticles with a size of roughly 20 nm. The second step involved the fabrication and functionalization of prepared AuNPs with resveratrol by polyethylene glycol (PEG). Small and uniformly dispersed AuNPs-PEG-Res nanoparticles is typical of AuNPs colloidal dispersion [18].

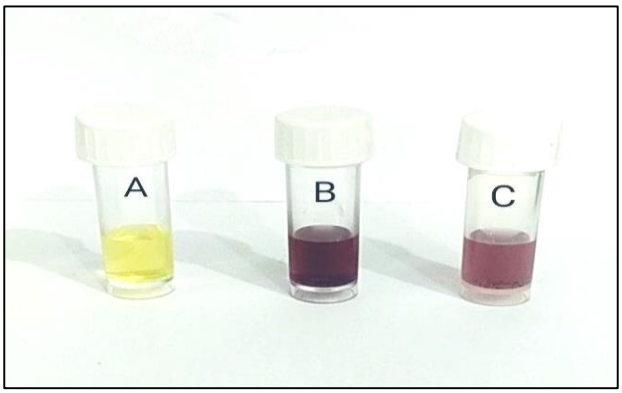

Figure (1): Gold nanoparticles (AuNPs) preparation. (A) Suspensions of gold salt solution ($HAuCl_4.3H_2O$). (B) Gold nanoparticles (AuNPs) and (C) functionalization of AuNPs with poly ethylene glycol (PEG) and Resveratrol (Res) (AuNPs-PEG-Res).

Characterization of AuNPs and AuNPs -PEG-Res

The UV–vis absorption spectra of gold nanoparticles are depicted in Figure (2). The higher absorption at 528 nm. Figure (2) (red line) showed the absorbance at 306 nm and 589 nm indicated the effective synthesis of AuNPs–PEG-Res. The chemical surfaces and functional group endpoints of AuNPs and AuNPs-PEG-Res were characterized using FT-IR spectroscopy (Figure 3). The spectra showed that there was an average of 20 scans made at a range of 4000 to 500 cm^{-1}.

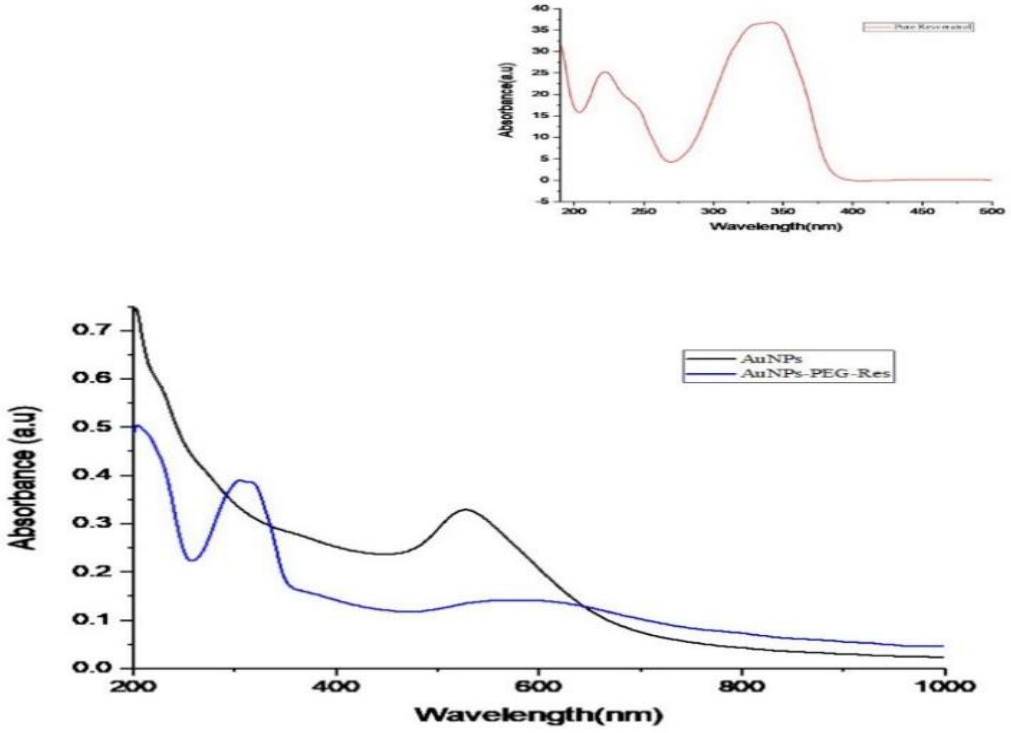

Figure (2): UV–vis absorption spectra of resveratrol (upper lane) AuNPs and AuNPs-PEG-Res (down lane). Experiments performed at room temperature

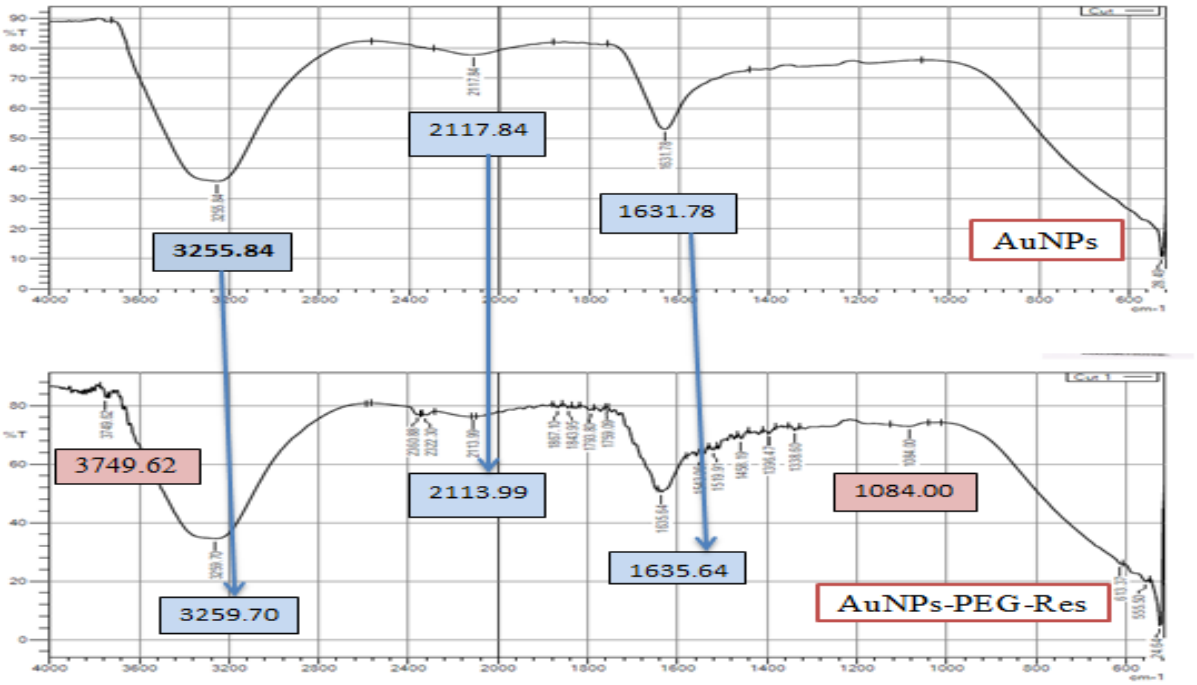

Figure (3): FT-IR analysis of AuNPs and AuNPs-PEG-Res. Experiments performed at room temperature.

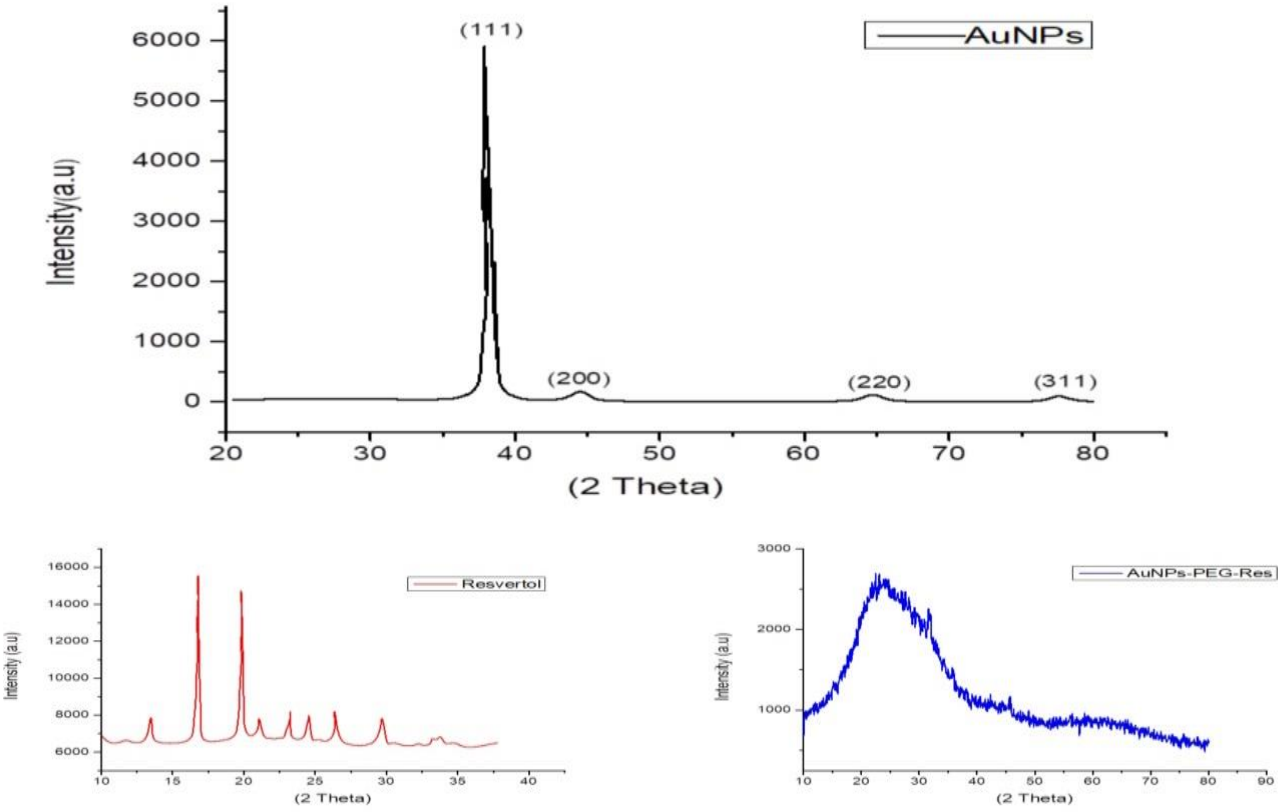

Figure (4): The XRD patterns of AuNPs, Resveratrol and AuNPs-PEG-Res.

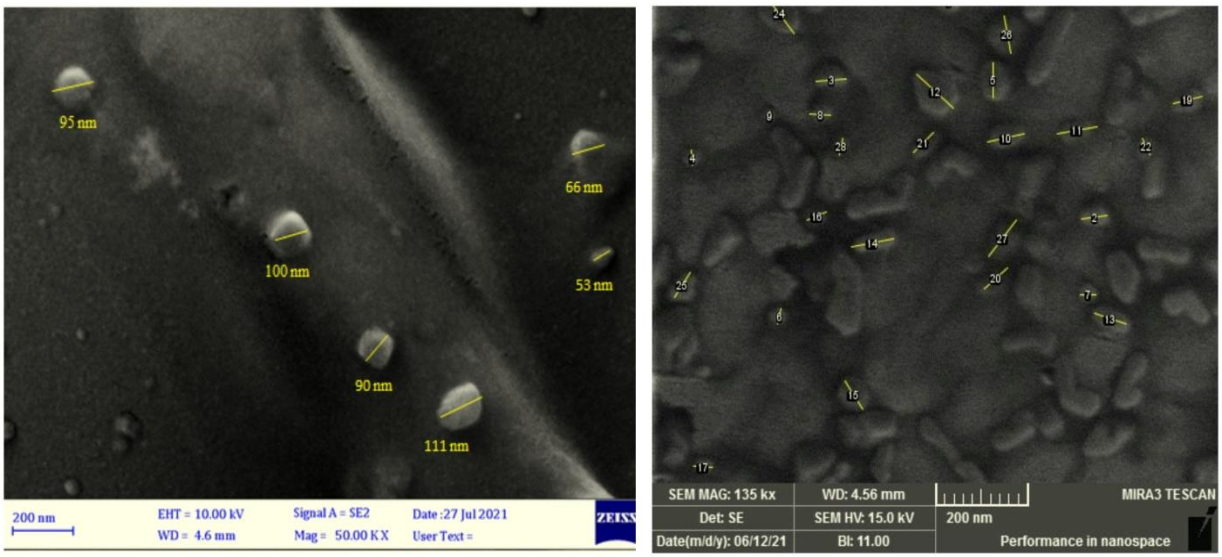

Figure (5): FE- SEM image of AuNPs (right lane) and FE- SEM image of AuNPs-PEG-Res (left lane) showing spherical and uniformly distributed nanoparticles .

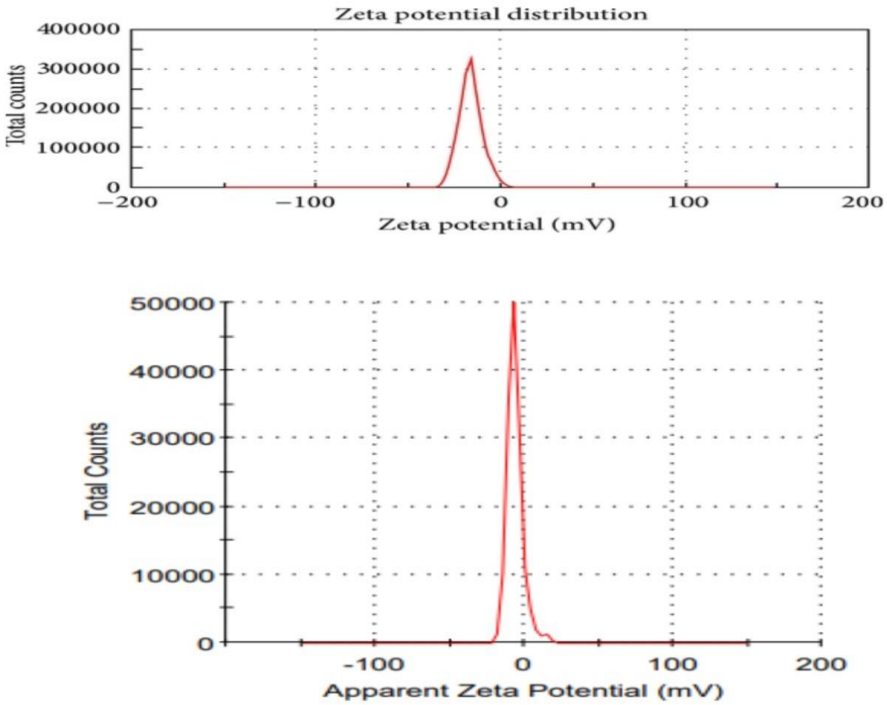

Figure (6): Zeta potential analysis for AuNPs, and AuNPs-PEG-Res.

Effect of AuNPs and AuNPs-PEG-Res on Serological parameters

Table (1) displayed the ELISA kit results for immune markers (**immunoglobulins** (IgA, IgE, IgG), autoantibodies (rheumatoid factor (RF), antinuclear antibodies (ANA), anti-double stranded DNA (Anti-dsDNA)), complement compounds (C3, C4), and interleukins (IL-6, and IL-33)). There was a significant reduction in the values of all these parameters in serum samples of RA patients ($P< 0.001$) when compared to the values of the healthy individuals group. Next, all the ten immune markers were evaluated to compare their levels in the serum samples of RA patients before and after AuNPs and AuNPs-PEG-Res exposure. The levels of all markers dropped rapidly in RA patients following exposure to AuNPs and AuNPs-PEG-Res, as compared to before exposure.

The reduction was highly significant ($P<0.001$) and serum levels of these markers were recovered to normality in the groups exposed to both types of nanoparticles (AuNPs and AuNPs-PEG-Res). The levels of IgE, RF, ANA, dsDNA, C3, C4, and IL-33 in the groups were lower after AuNPs exposure than after AuNPs-PEG-Res exposure.

Table (1): The immune markers (IgA, IgE, IgG, RF, ANA, Anti-dsDNA, C3, C4, IL-6, and IL-33) levels were compared between rheumatoid arthritis (RA) and healthy people.

Immune markers	Healthy people (n=20)	rheumatoid arthritis (n=20) P <0.001	Control (before exposing NPs) (n=28)	Exposing AuNPs (n=28) P <0.001	AuNPsPEG-Res (n=28) P <0.001
Immunoglobulin					
IgA	89.44± 52.17	277.97± 89.54	207.74±58.696	52.73±44.178,	36.09±10.373,
IgE	15.39± 13.46	64.25 ± 42.81	76.45±36.401	3.77±0.943,	6.14±5.453,
IgG	9.57± 2.64	189.65±101.74	153.12±57.24	16.94±23.25	8.71±2.98
Autoantibodies					
RF	114.11± 13.57	160.40± 29.87	166.12±22.88	91.64±14.14	107.88±22.65
ANA	0.20±0.05	0.68±0.20	0.65±0.17	0.13±0.1	0.16±0.03
Anti-dsDNA	0.20±0.02	0.54±0.22	0.58±0.15	0.16±0.08	0.18±0.03
Complement compounds					
C3	71.96±32.76	122.84 ±48.66	156.09±0.15	32.53±9.06	53.32±31.46
C4	35.80±16.20	58.03±23.35	71.19±22.79	16.43±5.28	20.08±8.01
Interleukins					
IL-6	22.89± 12.59	41.15± 8.28	39.60±8.07	12.33±3.57	12.50±5.98
IL-33	77.96± 52.31	252.69±120.54,	271.76±62.97	70.20±78.08	72.25±50.36

DISCUSSION

There was a progressive shift in coloring that progressed from pale yellow to bluish grey, purple, and finally red, indicating the creation of AuNPs. A model has been created for the citrate method of creating gold nanoparticles. It suggests that the oxidation of trisodium citrate to dicarboxy acetone converts Au^{+3} to Au^{+}. At the experiment temperatures, dicarboxy acetone breaks down. The disproportionation of Au^{+}, which is also accelerated by the gold surface, results in the creation of gold atoms, and it is this process that also causes growth. Dicarboxy acetone degradation has a significant impact on the rate of nucleation because nucleation necessitates the development of a multimolecular complex between dicarboxy acetone and AuCl. Also, **Kamal *et al.*** [19] reported that the presence of Res during the synthesis has no effect on the hydrophilic properties of the AuNPs and, on the contrary, makes them more stable. This is because they come into contact with more capping agents, such as cit, L-cys, and Res, which makes them smaller and the system more stable. The higher absorption at 528 nm in this study's absorbance spectra revealed that AuNPs were successfully synthesized. This is supported by the conclusions made by **Al-Dulimi *et al.*** [20] who reported that the absorbance peak of gold nanoparticles was 522 nm. The absorbance at 306 nm and 589 nm indicated the effective synthesis of AuNPs–PEG-Res. Prior observations by **Park *et al.*** [21] indicated the appearance of absorbance at 547 nm and successful synthesis of Res-AuNPs. Similarly, **Iswandana *et al.*** [17] observed ultraviolet-visible spectra of gold nanoparticles with a peak at 528.50 nm and AuNPs-PEG-Res absorbed light at 529 nm. The chemical surfaces and functional group endpoints of AuNPs and AuNPs-PEG-Res were characterized using FT-IR spectroscopy. The spectra demonstrated an average of 20 scans that observed at a range of 4000 to 500 cm^{-1}. The peak at 3255.84 cm^{-1} reflected an OH functional group along with an H-bounded vibration that was medium in strength. In addition, a detected peak at 2117.84 cm^{-1} was belonged to NH primary and secondary amines and amides that have higher strength, whereas that at 1631.78 cm^{-1} revealed a stretched C=O and deformed NH2 bonds in the primary amides. The peak at 1531 cm^{-1} was ascribed to gem-dimethyl, “iso” phenol or tertiary O-H group. The peaks in the range of 1400-1200 cm^{-1} of multiple aromatic (C=C) bonds were observed to have medium stretch vibrations. FTIR spectra of AuNPs-PEG-in the present study exhibited almost similar peaks as that of Res, indicating uniform deposition of Res over AuNPs. The only difference observed in the FTIR of AuNPs-PEG-Res over Res is the shift of a broad band observed

between 3259.70 cm^{-1}, 2113.99 cm^{-1} and 1635.64 cm^{-1}. The appearance of a peak observed at 3749.64 cm^{-1} is related to the PEG- (N–H) [17]. The strong diffraction peaks with 2θ values at 38.2º, 44.4º, 64.7º, and 77.7º are associated with the Bragg's reflections of 111, 200, 220, and 311 planes related to the face-centered cubic (FCC) of AuNPs. The diffraction peaks found were identical to those reported for the standard gold metal (Au^0). All of the AuNPs-PEG-Res diffraction peaks were found in the AuNPs. This showed that the AuNPs structure is stable in the presence of PEG-Res. Scherrer's formula is used to determine the crystalline size of Au nanoparticles. Relation:

$$\mathbf{D = 0.89\lambda/\beta \cos \theta}$$

The AuNPs appeared as smooth structures with good separation and a spherical, rod form with a size ranged from 33 to 361 nm. There were no aggregations and almost all of the particles had a single distribution with obvious homogeneity. This might result from the reduction of AuNP citrate in a polar solvent. Citrate ions may negatively charge the surface of AuNPs, which makes it easy for them to spread out [22]. FE-SEM image of an AuNPs-PEG-Res sample with spherical particles ranged in size from 49 to 157 nm. All of the nanoparticles were well separated and did not stick together or form clusters. This showed for sure that the resveratrol-capping has stabilized each nanoparticle.

The average size of AuNPs was 20 nm (Figure 6: upper side). The zeta potential of NPs varies depending on their surface chemistry. AuNPs had an average size of 20 nm. The zeta potential of NPs varies depending on their surface chemistry. Due to the presence of citrate molecules at their surface, which were used as a reducing agent during the production process, uncoated AuNPs possessed a negative surface charge (-34 mV). The AuNPs-PEG-Res had a smaller mean particle size, which could be attributed to the difference in components employed in its synthesis. AuNPs-PEG-Res possessed a negative surface charge (-20.7 mV), which shows that it is very stable. stating that the zeta potential should be >30 mV or <−30 mV to which shows that it is very stable. Gold compounds have been characterized as having an immunosuppressive impact by decreasing the production of pro-inflammatory cytokines such as TNF-, IL-6, and IL-1 [23]. Poly lactic-co-glycolic acid (PLG) nanoparticles actively transport therapeutic payloads to RA joints while blocking inflammatory cytokines. The high accumulation and lengthy retention of biomimetic nanocarriers in inflamed joints after intravenous injection resulted in good therapeutic effects [24].

After AuNPs exposure, the levels of IgA, IgE, IgG, ANA, Anti-dsDNA, C3, C4, and IL-6 in the groups were lower than after AuNPs-PEG-Res exposure. It is common knowledge that size is significant. It was discovered that smaller NPs were more likely to enter cells through endocytosis or diffusion, but larger NPs were more likely to enter cells through phagocytosis [25]. Two factors control how quickly and how many nanoparticles enter the cellular compartment via wrapping: the quantity of free energy produced by ligand-receptor interactions and the kinetics of receptor diffusion onto the wrapping sites on the cellular membrane [26]. **Huang *et al.*** [27] recently demonstrated that this outcome is most likely due to the particular benefits of nanoparticles smaller than 10 nm in terms of their capacity to interact with cells. It has been found that the surface properties of smaller AuNPs differ from those of larger nanomaterials. These differences are frequently represented in variations in the frequency and intensity of the corresponding surface plasmon resonance peaks.

However, the levels of IgA, IgG, and IL-6 in the group were lower after AuNPs-PEG-Res exposure than after AuNPs exposure. Res are potent anti-inflammatory and antioxidant substances that activate the sirtuin 1 (Sirt1), a NAD-dependent deacetylase that inhibits the transcription of adipogenic factors including PPARg and C/EBPa. **Harikumar *et al.*** [28] in RA patients discovered that downregulation of SIRT1 decreased the expression of inflammatory mediators cytokines. This significantly affects how the disease develops and progresses controlling. In the arthritis-induced mouse model, dietary supplementation of Res was reported to reduce the levels of TNF-a, IL-1b, IL-6, and soluble nuclear factor kappa B ligand.

After being exposed to AuNPs and AuNPs-PEG-Res, IgA, IgE, IgG, RF, ANA, and dsDNA levels were reduced rapidly in RA patients. The antigen-binding fragment (Fab), which recognizes the antigen, or the crystallizable fragment (Fc), which interacts with other immune system components, like phagocytes or complement pathway components, to promote antigen removal, may be responsible for antibody destruction in various regions of their structure. There has been no prior research to our knowledge that has investigated the roles of nanoparticle in RA management. Oriented covalent binding may boost antibody stability and control the accessible protein binding sites by binding to the Fc region, while leaving the antigen-binding site Fab region oriented to the medium in a ratio of one to one. It is advantageous if the attachment of the antibody to the nanoparticle via its Fc region is relatively simple, without affecting antibody activity, stable in high ionic concentration solutions, and allows for a high antibody load per nanoparticle. The direct attachment of the antibody's fragments (Fab) to the surface of the nanoparticles is another option where a precise orientation of the antibody is not required [29].

Numerous interfacial dynamic forces and physicochemical factors complicate and control the interaction between nanoparticles and complement proteins. Examples include surface imperfections and defects, functional groups and their surface densities, polymeric decorations, and architectural displays. To prevent complement activation and death, as well as to thwart complement-mediated opsonization processes, several pathogens have created and put into practice sophisticated surface and interfacial strategies. It the important to understand these events for designing and making nanomedicines that are safe for the immune system and can be used in the clinic. Complement proteins attach to the surface of nanoparticles after being intravenously administered into mice, a process known as opsonization [(30)]. High NP-protein affinities have been shown to cause bigger protein conformational changes, which increase the irreversibility of adsorption and conformational states. This begs the question whether if a protein adsorbs to a nanoparticle, a change in shape can render it inactive or at the very least, impair its function. Finally, the interaction of proteins with nanoparticles may suppress or enhance protein function [(31)].

Reducing the generation of pro-inflammatory cytokines is the main goal of current RA treatment plans. Additionally, *in vivo* therapeutic effect experiments revealed that the inhibition of pro-inflammatory cytokine release by the manufactured nanosystem has positive therapeutic effects for rats with AIA. More and more data points to the possibility that NPs can attach proteins to their surfaces. These interactions have a variety of effects. It's possible that neither the protein function nor the particle characteristics and subsequent toxicity are impacted by the protein/particle interaction. Alternately, the particles' surface reactivity may cause them to alter or disrupt the protein's structure, which would reduce its functionality. A different hypothesis is that protein binding changes the particle surface, lowering or changing its activity and the biological activity that results. Finally, the particles' large surface areas allowed them to bind a quantity of a particular protein [(32)].

CONCLUSION

Our study found that IgA, IgE, IgG, RF, ANA, Anti-dsDNA, C3, C4, IL-6, and IL-33 levels decreased rapidly in RA patients' sera and that a significant association between the patient groups ($P < 0.001$) was significantly higher than the control after AuNPs and AuNPs-PEG-Res exposure.

Conflict of interest: Nil
Sources of finding: Nil
Author contribution: Nil

REFERENCE

1. **Sampoorna M, Bhavani V, Ponnakanti K *et al.* (2020):** Ortholord Tablets: Nutritional Support for Rheumatoid Arthritis. Mediterranean Journal of Basic and Applied Sciences (MJBAS), 4 (2): 29-40.
2. **Guo Q, Wang Y, Xu D *et al.* (2018):** Rheumatoid arthritis: pathological mechanisms and modern pharmacologic therapies. Bone research, 6 (1): 1-14.
3. **Smolen S, Landewé R, Bijlsma J *et al.* (2017):** EULAR recommendations for the management of rheumatoid arthritis with synthetic and biological disease-modifying antirheumatic drugs: 2016 update. Annals of the rheumatic diseases, 76 (6): 960-977.
4. **Kasiotis K, Pratsinis H, Kletsas D *et al.* (2013)**: Resveratrol and related stilbenes: their anti-aging and anti-angiogenic properties. Food and Chemical Toxicology, 61: 112-120.
5. **Urbaniak A, Delgado M, Kacprzak K *et al.* (2017):** Activity of resveratrol triesters against primary acute lymphoblastic leukemia cells. Bioorganic & Medicinal Chemistry Letters, 27 (12): 2766-2770
6. **Li R, Li S, Lin C *et al.* (2018):** Effect of resveratrol and pterostilbene on aging and longevity. Biofactors, 44 (1): 69-82.
7. **Yahfoufi N, Alsadi N, Jambi M, *et al.* (2018):** The immunomodulatory and anti-inflammatory role of polyphenols. Nutrients, 10 (11): 1618.
8. **Saleh A (2020)**. Nanomaterials: Classification, properties, and environmental toxicities. EnvironmentalTechnology & Innovation, 20: 101067.
9. **Karak N (2019):** Fundamentals of nanomaterials and polymer nanocomposites. In Nanomaterials and polymer nanocomposites. https://www.researchgate.net/publication/330051923_Fundamentals_of...
10. **Koushki K, Keshavarz S, Keshavarz M *et al.* (2021):** Gold nanoparticles: Multifaceted roles in the management of autoimmune disorders. Biomolecules, 11 (9): 1289.
11. **Bromma K , Chithrani B (2020):** Advances in gold nanoparticle-based combined cancer therapy. Nanomaterials, 10 (9): 1671.
12. **Boyles S, Kristl T, Andosch A, Zimmermann M *et al.* (2015):** Chitosan functionalization of gold nanoparticles encourages particle uptake and induces cytotoxicity and pro-inflammatory conditions in phagocytic cells, as well as enhancing particle interactions with serum components. Journal of nanobiotechnology, 13 (1): 1-20.
13. **Li X, Wang H, Zou X *et al.* (2022):** Methotrexate-loaded folic acid of solid-phase synthesis conjugated gold nanoparticles targeted treatment for rheumatoid arthritis. European Journal of Pharmaceutical Sciences, 170: 106101.
14. **Yang G, Chang C, Yang Y *et al.* (2018):** Resveratrol alleviates rheumatoid arthritis via reducing ROS and inflammation, inhibiting MAPK signaling pathways, and suppressing angiogenesis. Journal of agricultural and food chemistry, 66 (49): 12953-12960.
15. **Nogueira E, Gomes A, Preto A *et al.* (2016):** Folate-targeted nanoparticles for rheumatoid arthritis

therapy. Nanomedicine: Nanotechnology, Biology and Medicine, 12 (4): 1113-1126.

16. **Turkevich C, Stevenson J, Hillier A *et al.* (1951):** study of the nucleation and growth processes in the synthesis of colloidal gold Discuss. Faraday Soc., 11: 55-75
17. **Iswandana R, Nurselviana R, Sutriyo S *et al.* (2020):** Synthesis and stability of resveratrol-conjugated gold nanoparticles modified with polyethylene glycol. International Journal of Applied Pharmaceutics, 12: 230-236.
18. **Kumar S, Gandhi S, Kumar R *et al.* (2007):** Modeling of formation of gold nanoparticles by citrate method. Ind Eng Chem Res., 46: 3128-36.
19. **Kamal R, Chadha D, Dhawan K *et al.* (2018):** Physiological uptake and retention of radiolabeled resveratrol loaded gold nanoparticles (99mTc-Res-AuNP) in colon cancer tissue. Nanomedicine: Nanotechnology, Biology and Medicine, 14 (3): 1059-1071.
20. **Al-Dulimi G, Al-Saffar Z, Sulaiman M *et al.* (2020):** Immobilization of l-asparaginase on gold nanoparticles for novel drug delivery approach as anti-cancer agent against human breast carcinoma cells. Journal of Materials Research and Technology, 9 (6): 15394-15411.
21. **Park S, Cha H, Cho I *et al.* (2016):** Antibacterial nanocarriers of resveratrol with gold and silver nanoparticles. Materials Science and Engineering, 58: 1160-1169.
22. **Crowley C, Marfell J, Waterhouse J *et al.* (2016):** Analyzing cell death by nuclear staining with Hoechst 33342. doi:10.1101/pdb.prot087338.
23. **Bondeson J (1997):** The mechanisms of action of disease-modifying antirheumatic drugs: a review with emphasis on macrophage signal transduction and the induction of proinflammatory cytokines. General Pharmacology: The Vascular System, 29 (2): 127-150.
24. **Wang Q, Qin X, Fang J, Sun X *et al.* (2021):** Nanomedicines for the treatment of rheumatoid arthritis: State of art and potential therapeutic strategies. Acta Pharmaceutica Sinica B, 11 (5): 1158-1174.
25. **Wu M, Guo H, Liu L *et al.* (2019):** Size-dependent cellular uptake and localization profiles of silver nanoparticles. International journal of nanomedicine, 14: 4247.
26. **Rahman A, Aziz A, Shamsuddin S *et al.* (2019):** The Effect of Gold Nanoparticle Size in the Cellular Uptake. In Solid State Phenomena. https://www.researchgate.net/profile/Shaharum-Shamsuddin/publica…
27. **Huang, X, El-Sayed M (2010):** Gold nanoparticles: Optical properties and implementations in cancer diagnosis and photothermal therapy. Journal of advanced research, 1 (1): 13-28.
28. **Harikumar B, Aggarwal B (2008):** Resveratrol: a multitargeted agent for age-associated chronic diseases. Cell cycle, 7 (8): 1020-1035.
29. **Marques C, Costa J, Velho S *et al.* (2020):** Functionalizing nanoparticles with cancer-targeting antibodies: A comparison of strategies. Journal of Controlled Release, 320: 180-200.
30. **Tomak A, Cesmeli S, Hanoglu D *et al.* (2021):** Nanoparticle-protein corona complex: understanding multiple interactions between environmental factors, corona formation, and biological activity. Nanotoxicology, 15 (10): 1331-1357.
31. **Brown M, Dickson C, Duncan P *et al.* (2010):** Interaction between nanoparticles and cytokine proteins: impact on protein and particle functionality. Nanotechnology, 21 (21): 215104.
32. **Manzanares D, Ceña V (2020):** Endocytosis: the nanoparticle and submicron nanocompounds gateway into the cell. Pharmaceutics, 12 (4): 371.